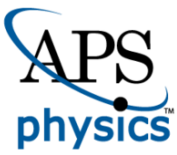

Ultrafast Electric Field Pulse Control of Giant Temperature Change in Ferroelectrics

Y. Qi, S. Liu, A. M. Lindenberg, and A. M. Rappe

Phys. Rev. Lett. **120**, 055901 — Published 30 January 2018

DOI: 10.1103/PhysRevLett.120.055901

Ultra–fast electric field pulse control of giant temperature change in ferroelectrics

Y. Qi,[1] S. Liu,[2] A. M. Lindenberg,[3,4] and A. M. Rappe[1]

[1]*The Makineni Theoretical Laboratories, Department of Chemistry, University of Pennsylvania, Philadelphia, PA 19104-6323, United States*

[2]*Geophysical Laboratory, Carnegie Institution for Science, Washington, D.C. 20015, United States*

[3]*Department of Materials Science and Engineering, Stanford University Stanford, CA 94305, United States*

[4]*PULSE institute, SLAC National Accelerator Laboratory, Menlo Park, CA 94025, United States*

(Dated: September 8, 2017)

Abstract

There is a surge of interest in developing environmentally friendly solid–state based cooling technology. Here, we point out that a fast cooling rate ($\approx 10^{11}$ K/s) can be achieved by driving solid crystals to a high–temperature phase with a properly designed electric field pulse. Specifically, we predict that an ultrafast electric field pulse can cause a giant temperature decrease up to 32 K in $PbTiO_3$ occurring on few picosecond time scales. We explain the underlying physics of this giant electric–field–induced temperature change with the concept of internal energy redistribution: the electric field does work on a ferroelectric crystal and redistributes its internal energy, and the way the kinetic energy is redistributed determines the temperature change and strongly depends on the electric field temporal profile. This concept is supported by our all–atom molecular dynamics simulations of $PbTiO_3$ and $BaTiO_3$. Moreover, this internal energy redistribution concept can also be applied to understand electrocaloric effect. We further propose new strategies for inducing giant temperature decrease with electric field pulse. This work offers a more general framework to understand electric field controlled temperature change and highlights the opportunities of electric–field engineering for controlled design of fast and efficient cooling technology.

Recent years have seen a surge of interest in developing solid–state–based cooling technology [4–8], which does not rely on the high global–warming potential refrigerants (hydrofluorocarbons and hydrochlorofluorocarbons) that are widely used in traditional vapor compression cooling technology. The electrocaloric effect (ECE), which refers to the phenomenon in which the temperature of a material changes reversibly under the application and removal of an electric field [1–3], is a promising solid-state cooling technique. Giant positive ECEs up to 12 K have been observed in $PbZr_{0.95}Ti_{0.05}O_3$, and paving the path toward the practical application of the ECE is a fast–moving research project [9]. Similar to a mechanical refrigeration cycle, the traditional ECE–based refrigeration cycle involves four steps: (1) the temperature of a crystal increases under the application of electric field; (2) the crystal ejects heat to a sink; (3) the electric field is removed, and the temperature of the crystal decreases; (4) the crystal is contacted with a load and adsorbs heat from it [10].

It is generally assumed the temperature decrease during the electric field removal should equal the temperature increase during the electric field application [11]. However, sometimes the cooling is less than expected, or even cannot be observed [7, 12–14]. The reasons include but are not limited to: the dielectric loss during the polarization relaxation, friction during the transfer of the crystal from the hot sink to the cold load, and entropy production during an irreversible process [12–15]. Therefore, an effect, in which the temperature of a material will decrease (rather than increase) in response to an electric field, is significantly more desired for effectively cooling the load [11, 12, 16].

In this work, we focus on a new Electric field Pulse–Induced Temperature Change (EPITC) phenomenon, in which temperature can decrease right after the application of an electric pulse. Different from conventional ECE, EPITC is induced by just a single electric field pulse and is an irreversible process. However, ECE and EPITC share the same physical mechanism, electric field disorders or aligns local polarization in ferroelectrics, and causes change in structure and temperature. Therefore, in this study, we start by clarifying the mechanism underlying both EPITC and ECE from the energy conservation point of view. The external electric field does work on a ferroelectric crystal and causes structural change, accompanied with a modification in potential energy. As a result, the kinetic energy, which relates to the temperature, also changes accordingly. The signs and magnitudes of these changes are determined by the electric field profile. Based on this improved understanding, we demonstrate that negative and giant temperature decrease in prototypical ferroelectric

$PbTiO_3$ can be realized with short electric field pulses, which correspond to giant cooling rates.

The ECE has been widely understood as entropy reallocation [2, 5, 11]. The application of an electric field aligns dipoles in a material, and the configurational entropy is reduced. As a result, the thermal entropy, which corresponds to the lattice vibrations, increases. This mechanism only holds for a reversible adiabatic process, which requires the system to be at equilibrium throughout. Real adiabatic process rarely exists in practice. For a ferroelectric system with thermal hysteresis, the entropy production is unavoidable in a loop. The dielectric loss and friction mentioned before also cause entropy production. Because of the insufficiencies in explaining ECE in ferroelectrics with entropy reallocation, we propose that it is much more straightforward to understand the ECE and EPITC with the concept of internal energy U (per unit volume) redistribution. Here, we should emphasize that from our MD simulation, the volume change is quite small (less than 1%). Therefore, the mechanical work is negligible, and the internal energy is very close to the enthalpy. The work W (per unit volume) done by the electric field E is given as

$$W = \int \boldsymbol{E} \cdot \mathrm{d}\boldsymbol{P} \tag{1}$$

where $\boldsymbol{P}$ is the macroscopic polarization of the material at finite T. It is generally assumed that ECE and EPITC occurs in a short period of in the absence of heat transfer [7, 11]. Therefore, the internal energy change ΔU is equal to the electrical work:

$$\Delta U = \Delta U_k + \Delta U_p = W \tag{2}$$

where ΔU_k and ΔU_p are changes in kinetic energy and potential energy. The temperature change ΔT is associated with ΔU_k as

$$\langle \Delta U_k \rangle = \frac{3}{2} k_B \Delta T N \implies \Delta T \propto \langle \Delta U_k \rangle \tag{3}$$

where N is the number of atoms per unit volume, k_B is the Boltzmann constant, and $\langle \Delta U_k \rangle$ denotes the ensemble average of the kinetic energy change ΔU_k. Generally, the direction of the polarization change $\mathrm{d}\boldsymbol{P}$ is along that of the applied electric field, and therefore W is positive. In most cases, the applied electric field induces a more polar structure, which possesses lower potential energy for ferroelectric materials ($\Delta U_p < 0$). Therefore, $\Delta U_k = W - \Delta U_p$ is usually positive when turning on the electric field and negative when removing the electric field, causing heating and cooling respectively.

However, ΔU_k could be negative upon electric field application, thus giving rise to negative ECE and EPITC, in which the temperature decreases right after the application of electric field. For example, when there is a field–induced phase transition with positive transition energy $U_{\rm tr}$ (the difference between the potential energies of the two phases per unit volume). In this case, $\Delta U_p \approx U_{\rm tr}$, and if $W < U_{\rm tr}$, we have $\Delta U_k = W - U_{\rm tr} < 0$. That is some kinetic energy goes to compensate the transition energy, and the temperature decreases.

Negative EPITC is significant because it can offer a fast, direct and efficient cooling technique [11, 12, 16–18], where cooling is achieved through the application of electric field. It is one of the rare cases where doing work on a system causes its temperature to decrease. Here, we perform NPT (isobaric–isothermal) MD simulations with bond–valence–model based interatomic potentials, which have been proven reliable in simulating structural properties and dynamics of ferroelectrics under various conditions [19–23], to illustrate the theory of negative EPITC in a realistic context. 10×10×10 supercells (5000 atoms) were used for both $BaTiO_3$ and $PbTiO_3$. The temperature was controlled via the Nosé–Hoover thermostat [24, 25] and the pressure was maintained at 1 atm via the Parrinello–Rahman barostat [26]. Each simulation was performed with a 0.5 fs time step. For simulating equilibrium states, the thermal inertia M_s, which is the mass of the thermostat that controls the speed of heat transfer, was selected as 1.0 amu, in order to control the temperature effectively [24, 25]. Adiabatic MD simulations for the pulse application or removal began with equilibrated states, and M_s was set with a large value (50000), in order to prohibit heat transfer [11]. Therefore, these simulations are adiabatic, aiming to describe the structural and temperature change during the short pulse period, rather than isobaric–isothermal long–trajectory simulations, which describe the equilibrium states at a specific temperature and pressure. The parameters of the bond valence model, the method of calculating local polarization, and the phase transition temperatures given by this model are described in references [18, 22]. It is also worth mentioning that the transition temperatures are usually underestimated in our bond–valence model. However, this would not greatly affect the applicability of this potential [19–23], and the mechanisms of such underestimations are given in references [18, 22]. For practical application, these temperatures could be scaled.

At 101 K, the $BaTiO_3$ crystal is in its rhombohedral phase in our MD simulations. An electric field along the (110) direction is applied to drive the system from the rhombohedral

to the orthorhombic phase. As shown in Fig. 1 (a), the polarization components along the x and y directions (P_x and P_y, parallel to E) increase slightly ($\Delta P_i = 0.04$ C/m^2), indicating that the work W done by the electric field E is small. The crystal is driven to the orthorhombic phase, accompanied by an increase of the potential energy, because there is a transition energy $U_{\rm tr}$ for the rhombohedral to orthorhombic phase transition, as shown in Fig. 1 (a) and (b). Since

$$W \approx 0,\ \Delta U_p = U_{\rm tr} > 0, \tag{4}$$

$$\Delta U_k = W - \Delta U_p < 0, \tag{5}$$

we observe in MD simulations a decrease in temperature, with an ultra–fast cooling rate ($\approx 10^{11}$ K/s). Based on equation (5), we can estimate the upper limit of electric field $E_{\rm max}$ causing temperature decrease in our BTO MD model:

$$W - \Delta U_p < 0,\ \boldsymbol{E_{\rm max}}\cdot\Delta\boldsymbol{P} < U_{\rm tr} \tag{6}$$

$$E_{{\rm max},i} < \frac{U_{\rm tr}}{\Delta P_i} \approx 800 \text{ kV/cm}. \tag{7}$$

Similarly, we can also realize a negative EPITC through the orthorhombic to tetragonal phase transition. The case for tetragonal to cubic phase transition is less straightforward, because no unidirectional quasi–static electric field can induce the tetragonal to cubic phase transition. Previous studies demonstrate that the cubic phase of $BaTiO_3$ crystal has a disorder character [27–29]; the dipoles in various unit cells orient in different directions and vary with time, and the macroscopic polarization is zero [18]. Here, we design a single cycle terahertz pulse [30, 31] which is perpendicular to the polarization. A rapidly oscillating electric field pulse can disorder the polarization, effectively changing the system to the cubic phase. The post–pulse state behaves as a supercooled cubic phase. The temperature decrease due to tetragonal–cubic transition in BTO is larger ($\approx$ 2 K) than that due to orthorhombic–tetragonal transition, as shown in Fig. 2 (a), which is directly related to the larger transition energy of the tetragonal–cubic phase transition. We highlight that the negative EPITC requires the occurrence of a phase transition. In the absence of field–driven phase transition, because of the one–to–one relationship between internal energy and temperature in the same phase, the system with higher energy will have higher temperature.

From the analysis above, we demonstrate that negative EPITC can be achieved with electric field–induced phase transitions from the low–temperature phase to the high–temperature

phase, because some of the kinetic energy is lost to compensate the potential energy increase. Conversely, if the transition is from high–temperature phase to low–temperature phase, temperature increases and we find positive EPITC. In Fig. 3, we plot the temperature changes of $BaTiO_3$ and $PbTiO_3$, under the application of a 600 kV/cm electric field. We observe ΔT = 9.0 K, 50.0 K respectively for $BaTiO_3$ and $PbTiO_3$. The temperature change (for the same electric field) for $PbTiO_3$ is giant and about five times of that for $BaTiO_3$. This is attributed to its larger transition energy (five times that of $BaTiO_3$).

We also predict large negative EPITC in $PbTiO_3$. An ultra–fast electric–field pulse is applied anti–parallel to the $PbTiO_3$ polarization, as shown in Fig. 2 (b). This electric–field pulse induces some negative local polarization in a positively polarized crystal. This does work $W = \int \boldsymbol{E} \cdot \mathrm{d}\boldsymbol{P} > 0$. The polarization evolution in the Gibbs free energy profile is shown in Fig. 4. After the pulse, the system passes the energy barrier between the tetragonal and cubic phases, and the system evolves to a local minimum corresponding to cubic phase without any external force. As expected, this electric field pulse induces a tetragonal–to–cubic phase transition, and a 32 K temperature decrease is observed, which is much higher than recent experimental observations [32–36]. This supercooled cubic phase crystal could potentially be used in a cooling cycle. After adsorbing heat and equilibrating with a load, the crystal is contacted with a sink. Application of a quasi–static electric field can drive it back to its original phase with a higher temperature, and then the crystal gives off heat and cools to its original state.

These results indicate that a large transition energy is critical for giant EPITC. The transition energy sets the upper limit for negative EPITC, according to equations (3) and (5):

$$\Delta T_{\max} = \frac{2U_{\mathrm{tr}}}{3k_B N}. \tag{8}$$

Gibbs free energy, which takes entropy into consideration, reflects the stability of a specific phase at a certain temperature [37, 38]. It should be emphasized that a triple well Gibbs free energy landscape, as shown in Fig. 4, is necessary for such negative EPITC. This requires the operating temperature being close to the Curie temperature T_C. Around T_C, the free energies of the polar and non–polar states are so close that the driving force for polar domain wall nucleation and growth is very low. As a result, the applied electric field pulse tends to disrupt the local polarization and trigger the phase transition, rather than induce domains. Our simulations demonstrate that the metastable cubic phase of $PbTiO_3$ can last for a long

period of time (more than 20 ns), which is long enough for heat transfer. This is because the transition from a metastable cubic structure to a tetragonal one begins with the nucleation of a small region with local parallel polarization. However, the formation of a polar nuclei in a non–polar matrix costs domain wall energy, which is unfavorable around T_C [23, 39], as demonstrated in Fig. 4. In summary, we desire two phases with a large difference in potential energy, in order to acquire large temperature change, and a small difference in Gibbs free energy, so that the metastable high–temperature phase lasts a long time and can be induced by an electric field pulse.

Though $PbTiO_3$ exhibits a giant EPITC effect near T_c, its high T_c (765 K in experiments) may impede practical applications at room temperature [40]. Techniques that can suppress T_c of $PbTiO_3$–based ferroelectrics such as doping and strain engineering will be helpful for developing practical negative EPITC materials [41]. Another practical concern is that Joule heating may counteract negative EPITC. Joule heating depends on the conductivity of the sample and the field duration, and the conductivity of prototypical ferroelectrics could be affected significantly by soft–mode absorption at THz frequencies. A previous combined theoretical and experimental study demonstrates that for $BaTiO_3$ at THz frequencies, the dielectric loss calculated from first–principles based MD matches that acquired from experimental measurement [42], indicating that the soft–mode related conductivity of $BaTiO_3$ is included appropriately in MD simulations. Moreover, previous experiments also suggest that $PbTiO_3$, which we predict to show giant pulse–induced negative EPITC in this study, has low conductivity (and heating) under THz excitation. [43].

In this study, we analyze and explain ECE and EPITC from an energy point of view: the electric field does work on a crystal, reallocates its kinetic and potential energies, and causes temperature change. We propose that negative EPITC can be both ultra–fast and giant (T reduction as high as 32 K), and a low–temperature to high–temperature phase transition is required in such an giant and negative EPITC. The cooling rate due to pulse-induced negative EPITC is fast ($\approx 10^{11}$ K/s), because of the fast response of polarization in prototypical ferroelectrics to electric field (in picoseconds).

Y.Q. and A.M.R. were supported by the U.S. Department of Energy, under Grant No. DE–FG02–07ER46431. S.L. is supported by Carnegie Institution for Science. A.M.L. acknowledges support from the Department of Energy, Basic Energy Sciences, Materials Sciences and Engineering. The authors acknowledge computational support from the NERSC

of the DOE.

---

[1] M. C. Rose and R. E. Cohen, Phys. Rev. Lett. **109**, 187604 (2012).

[2] I. Takeuchi and K. Sandeman, Phys. Today **68**, 48 (2015).

[3] X. Moya, S. Kar-Narayan, and N. D. Mathur, Nat. Mater. **13**, 439 (2014).

[4] S.-G. Lu and Q. Zhang, Adv. Mater. **21**, 1983 (2009).

[5] M. Valant, Prog. Mater Sci. **57**, 980 (2012).

[6] L. Manosa, A. Planes, and M. Acet, J. Mater. Chem. A **1**, 4925 (2013).

[7] J. F. Scott, Annu. Rev. Mater. Res. **41**, 229 (2011).

[8] B. Neese, B. Chu, S.-G. Lu, Y. Wang, E. Furman, and Q. M. Zhang, Science **321**, 821 (2008).

[9] A. S. Mischenko, Q. Zhang, J. F. Scott, R. W. Whatmore, and N. D. Mathur, Science **311**, 1270 (2006).

[10] G. Akcay, S. P. Alpay, J. V. Mantese, and G. A. Rossetti, Appl. Phys. Lett. **90**, 2909 (2007).

[11] I. Ponomareva and S. Lisenkov, Phys. Rev. Lett. **108**, 167604 (2012).

[12] X. Qian, T. Yang, T. Zhang, L.-Q. Chen, and Q. M. Zhang, Appl. Phys. Lett. **108**, 142902 (2016).

[13] H. Gu, X. Qian, X. Li, B. Craven, W. Zhu, A. Cheng, S. C. Yao, and Q. M. Zhang, Appl. Phys. Lett. **102**, 122904 (2013).

[14] U. Plaznik, A. Kitanovski, B. Rožič, B. Malič, H. Uršič, S. Drnovšek, J. Cilenšek, M. Vrabelj, A. Poredoš, and Z. Kutnjak, Appl. Phys. Lett. **106**, 043903 (2015).

[15] U. Plaznik, M. Vrabelj, Z. Kutnjak, B. Malič, A. Poredoš, and A. Kitanovski, Europhys. Lett. **111**, 57009 (2015).

[16] R. Pirc, B. Rožič, J. Koruza, B. Malič, and Z. Kutnjak, EPL **107**, 17002 (2014).

[17] W. Geng, Y. Liu, X. Meng, L. Bellaiche, J. F. Scott, B. Dkhil, and A. Jiang, Adv. Mater. **27**, 3165 (2015).

[18] Y. Qi, S. Liu, I. Grinberg, and A. M. Rappe, Phys. Rev. B **94**, 134308 (2016).

[19] I. Grinberg, V. R. Cooper, and A. M. Rappe, Nature **419**, 909 (2002).

[20] Y.-H. Shin, I. Grinberg, I.-W. Chen, and A. M. Rappe, Nature **449**, 881 (2007).

[21] R. Xu, S. Liu, I. Grinberg, J. Karthik, A. R. Damodaran, A. M. Rappe, and L. W. Martin, Nat. Mater. **14**, 79 (2015).

[22] S. Liu, I. Grinberg, H. Takenaka, and A. M. Rappe, Phys. Rev. B **88**, 104102 1 (2013).

[23] S. Liu, I. Grinberg, and A. M. Rappe, Nature **534**, 360 (2016).

[24] W. G. Hoover, Phys. Rev. A **31**, 1695 (1985).

[25] S. Nosé, J. Chem. Phys. **81**, 511 (1984).

[26] M. Parrinello and A. Rahman, Phys. Rev. Lett. **45**, 1196 (1980).

[27] M. Gaudon, Polyhedron **88**, 6 (2015).

[28] K. Itoh, L. Zeng, E. Nakamura, and N. Mishima, Ferroelectrics **63**, 29 (1985).

[29] E. A. Stern, Phys. Rev. Lett. **93**, 037601 (2004).

[30] T. Qi, Y. H. Shin, K. L. Yeh, K. A. Nelson, and A. M. Rappe, Phys. Rev. Lett. **102**, 247603 1 (2009).

[31] F. Chen, J. Goodfellow, S. Liu, I. Grinberg, M. C. Hoffmann, A. R. Damodaran, Y. Zhu, P. Zalden, X. Zhang, I. Takeuchi, *et al.*, Adv. Mater. **27**, 6371 (2015).

[32] D. Guyomar, G. Sebald, B. Guiffard, and L. Seveyrat, J. Phys. D: Appl. Phys. **39**, 4491 (2006).

[33] G. Sebald, S. Pruvost, L. Seveyrat, L. Lebrun, D. Guyomar, and B. Guiffard, J. Eur. Ceram. Soc. **27**, 4021 (2007).

[34] S. G. Lu, B. Rozic, Q. M. Zhang, Z. Kutnjak, R. Pirc, M. Lin, X. Li, and L. Gorny, Appl. Phys. Lett. **97**, 202901 (2010).

[35] X. Moya, E. Stern-Taulats, S. Crossley, D. González-Alonso, S. Kar-Narayan, A. Planes, L. Mañosa, and N. D. Mathur, Adv. Mater. **25**, 1360 (2013).

[36] Y. Bai, G. Zheng, and S. Shi, Appl. Phys. Lett. **96**, 192902 (2010).

[37] J. Hlinka and P. Márton, Phys. Rev. B. **74**, 104104 (2006).

[38] L.-H. Ong, J. Osman, and D. R. Tilley, Phys. Rev. B **63**, 144109 (2001).

[39] W. J. Merz, Phys. Rev. **95**, 690 (1954).

[40] G. Shirane and S. Hoshino, J. Phys. Soc. Jpn. **6**, 265 (1951).

[41] G. A. Rossetti Jr, L. E. Cross, and K. Kushida, Appl. Phys. Lett. **59**, 2524 (1991).

[42] J. Hlinka, T. Ostapchuk, D. Nuzhnyy, J. Petzelt, P. Kuzel, C. Kadlec, P. Vanek, I. Ponomareva, and L. Bellaiche, Phys. Rev. Lett. **101**, 167402 (2008).

[43] C. H. Perry, B. N. Khanna, and G. Rupprecht, Phys. Rev. **135**, A408 (1964).

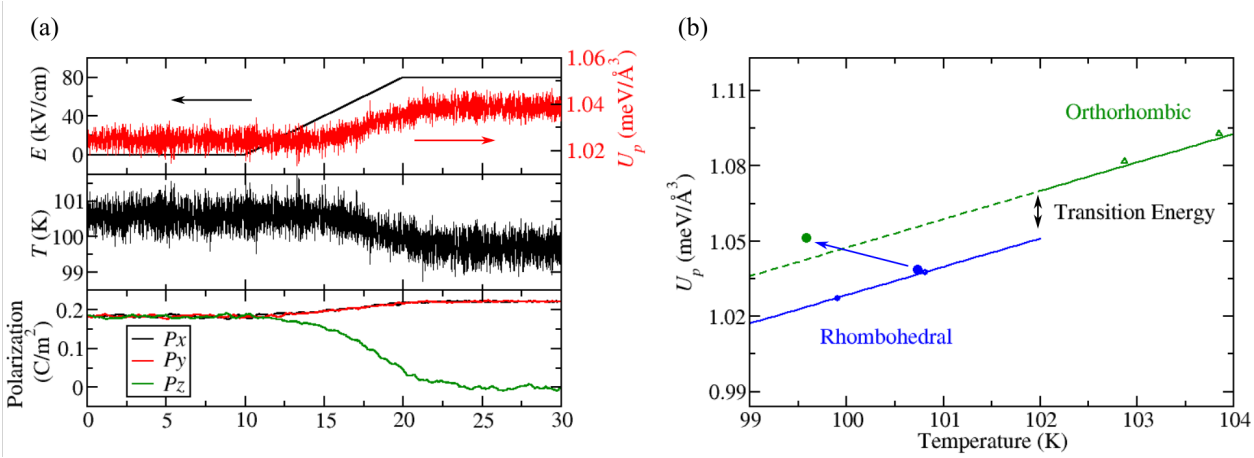

FIG. 1. Negative electrocaloric effect associated with the rhombohedral to orthorhombic phase transition in $BaTiO_3$. (a) Electric field, potential energy, temperature and polarization *vs.* time. The potential energy of the $T = 0$ K ground structure is set as the zero of potential energy. An 80 kV/cm electric field is applied along the (110) direction with $T = 101$ K. The electric field rises to its steady–state value within 5 ps, rather than instantaneously. This is chosen because for the negative EPITC, less work (W) and entropy production are preferred. In our MD simulations, the rhombohedral to orthorhombic phase transition occurs at 102 K under zero electric field and at 94 K under an 80 kV/cm electric field. Therefore, at 101 K, $BaTiO_3$ is at its rhombohedral phase under zero electric field and an 80 kV/cm electric field is large enough for triggering a rhombohedral to orthorhombic phase transition. (b) Schematic plot of potential energy *vs.* temperature for the two phases, demonstrating the electric field–induced phase transition and ultra–fast temperature reduction. The solid blue and green lines indicate the potential energies of equilibrated states at different temperatures. The blue and green circles represent the states before and after the application of electric field.

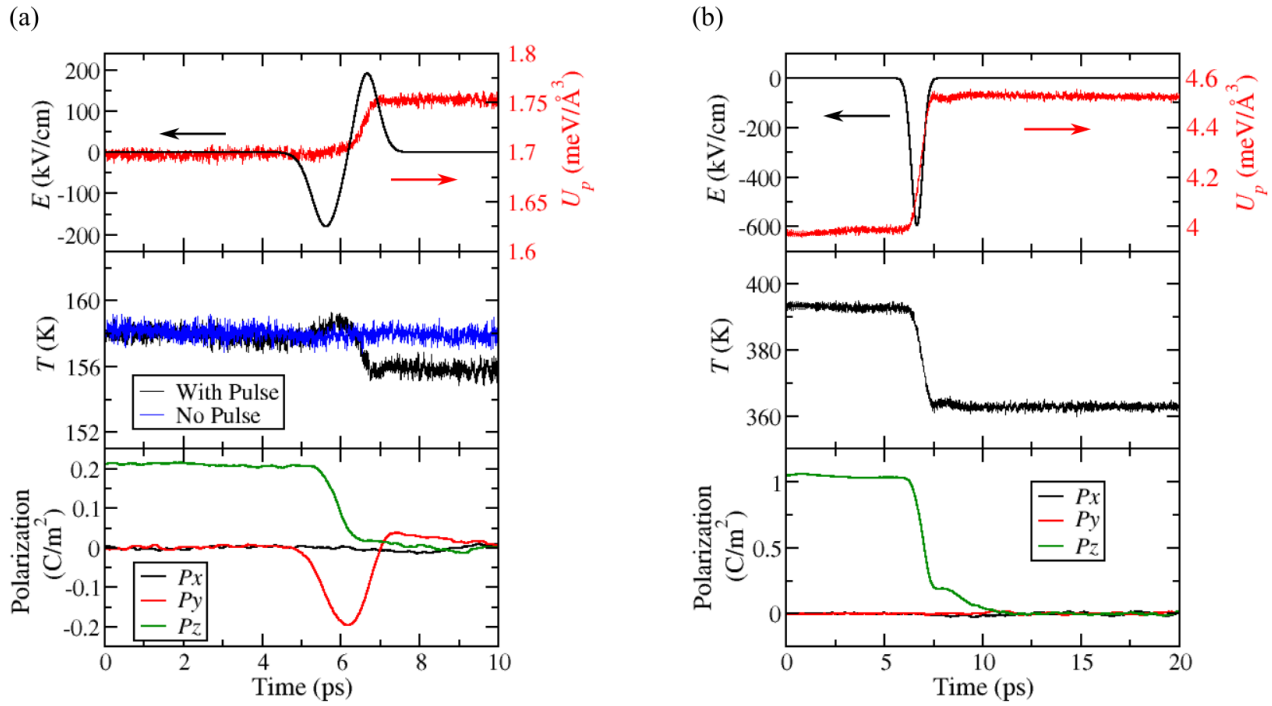

FIG. 2. Time evolution of the electric–field pulse, potential energy, temperature, and polarization along the three Cartesian axes for (a) $BaTiO_3$, under a single–cycle THz electric field pulse perpendicular to the polarization in tetragonal $BaTiO_3$. The tetragonal to cubic phase transition of $BaTiO_3$ under zero electric field occurs at 160 K in our MD simulation [18]. This pulse induces a tetragonal to cubic phase transition, which was demonstrated by both the potential energy and polarization profile. For the middle plot, the blue line indicates the temperature evolution under zero electric field pulse, as a comparison. (b) $PbTiO_3$, under a half–cycle THz electric field pulse anti–parallel to polarization in $PbTiO_3$. The tetragonal to cubic phase transition of $PbTiO_3$ under zero electric field occurs at 395 K in our MD simulation [22]. For $PbTiO_3$, the negative EPITC is giant (32 K), due to the large transition energy. For $BaTiO_3$ and $PbTiO_3$, we used electric field pulses with different profiles; actually, either of them works well in scrambling the local polarization, and they are similar in effectiveness. If we use a pulse with a full cycle, it should be perpendicular to the polar axis. This pulse will reorient the polarization first, and then flip parts of local polarization in this newly oriented polar direction. If a half–cycle pulse is selected, it should be anti–parallel to the polar direction, in order to reverse parts of local polarization and drive the crystal to a non–polar state.

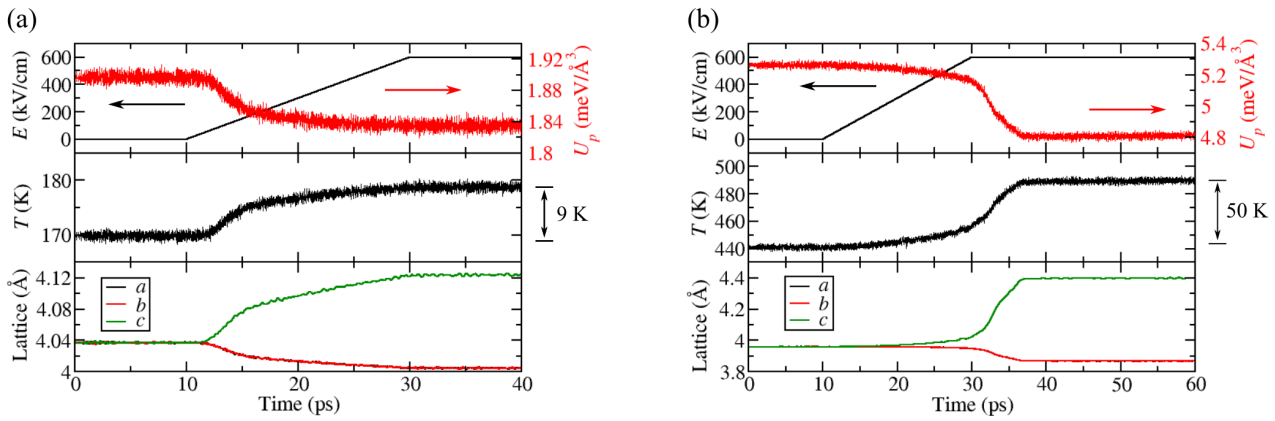

FIG. 3. Time evolution of the electric–field pulse, potential energy, temperature, and lattice constants for $BaTiO_3$ and $PbTiO_3$ under the application of a 600 kV/cm electric field. (a) Electric field is applied, and the $BaTiO_3$ crystal undergoes a cubic to tetragonal phase transition, with a 9 K temperature increase; (b) Electric field is applied on a $PbTiO_3$ crystal, causing a phase transition with a 50 K temperature increase.

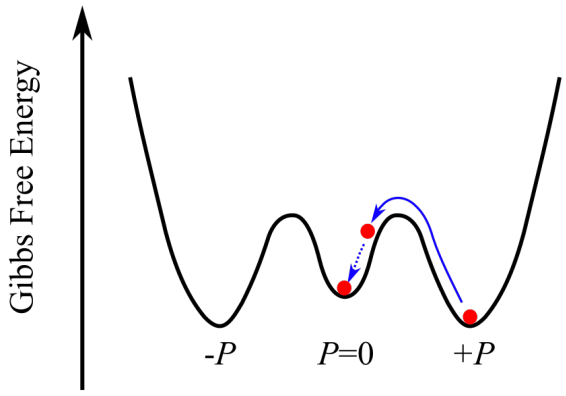

FIG. 4. Schematic representation of the polarization evolution in the Gibbs free energy profile. The outer two minima represent the states with positive and negative polarization. The central minimum represents a cubic phase. The solid blue curve represents that the electric–field pulse drives the ferroelectric crystal from its tetragonal phase toward the cubic, and over the energy barrier. The dashed blue curve indicates that the system evolves to the cubic phase after the pulse. For $PbTiO_3$, because the energy barrier in the Gibbs free energy profile, which relates to the energy required for polar nuclei formation and growth, is high at $T \approx T_C$, polar nuclei are slow to form and the system can be trapped in the cubic local minimum for nanoseconds, which is long enough for heat transfer. For $BaTiO_3$, the energy barrier between polar and non–polar states are much lower. As a result, the supercooled non–polar state can last for approximately 100 ps.